

THE DYNAMICAL CONTRIBUTION OF THE HALO MASS TO THE SPIRAL STRUCTURE

By

CH. K. TERZIDES

(Astronomy Department, Aristotelian University of Thessaloniki)

(Received 21.6.1980)

Abstract: *In this study the effects of halos on the dynamics of spiral structure are examined.*

Especially we make a classification of the rotation curves in galaxies and study the influence of a halo and of a central mass on the positions of the resonances and on the pitch angle of the spiral arms.

1. INTRODUCTION

The concept of massive halos of high-velocity stars has been suggested by Ostriker and Peebles (1973) (see also Ostriker et al. 1974, Ostriker and Thuan 1975) in order to stabilize a galactic disk of low-velocity stars, against bar-like instabilities observed in computer experiments (Miller 1974, Hohl 1975, Hockney and Brownrigg 1974). Ostriker and Peebles (1973) after a 3-dimensional numerical experiment, established a criterion according to which non axisymmetric instabilities are avoided only if the ratio of the total kinetic energy of rotation to the potential energy of the system is smaller than 0.14. This result means that at least 3/4 of the total kinetic energy are in random motions.

Observational evidence for massive halos in galaxies comes from estimates of the masses of galaxies by Einasto (Einasto et al. 1974a, b, Chernin, Einasto and Saar 1976) and from the rotation curves of some galaxies at large distances (Rubin and Ford 1970, Roberts and Rots 1973).

In the computer experiments that produce spiral waves, rather than material arms, the stars acquire finally large random velocities. It has been suggested by Miller (1974) that this fact is due to non-axisymmetric instabilities of a disk with low-velocity stars and is in-

dependent of the experimental conditions. The halo considered by Ostriker and Peebles (1973) could stabilize such a disk.

Among the computer experiments that have taken into account a halo component are those due to Hohl (1975) and Hockney and Brownrigg (1974). Hohl examined the results of a halo on barred spirals and the conditions under which this spiral structure can survive. Hockney and Brownrigg found that relatively long-lived apiral arms are observed when the proportion of population II stars in a galaxy is large.

In the present study we consider the effects of various assumed halos on the dynamics of spiral galaxies, under the assumption that the halo population does not interact with the disk, namely that it does not participate in the spiral arms. An application of this hypothesis is that the dispersion of velocities of the halo objects must be large.

As axisymmetric background we have used the model of Schmidt (1965) (called afterwards S-model) and the model proposed by Miyamoto and Nagai (1975) (called afterwards M-model).

a) S-model

The S-model consists of three parts:

- I. a central mass equal to $0.07 \times 10^{11} \odot$
- II. a spheroid with major semiaxis: $r_s = 9.73217283$ kpc, eccentricity: $e = 0.998749$ and ratio of axes 0.05 where the density follows the law:

$$\rho(r) = \frac{3.93}{r} - 0.02489 \text{ } r_{\odot}/\text{pc}^3 \quad (r < r_s) \quad (1)$$

and its total mass is $0.82 \times 10^{11} \odot$.

- III. A spheroidal shell surrounding the previous one with a density law:

$$\rho(r) = \frac{1449.2}{r} \odot/\text{pc}^3 \quad (r > r_s) \quad (2)$$

and mass $0.93 \times 10^{11} \odot$.

The total mass of the model is $1.8 \times 10^{11} \odot$.

According to the S-model, the force on the plane of symmetry, as a function of the galactocentric distance for $r < r_s$ is given by (Schmidt 1965):

$$F(r) = \frac{30000}{r^2} + 10120.2 - 41.722r^2 \text{km}^2 \text{sec}^{-2} \text{kpc}^{-1} \quad (3)$$

while for $r > r_s$ by (Contopoulos, 1975):

$$F(r) = \frac{4\pi \sqrt{1-e^2} 1449.2 G10^3}{r^3} \left[\left(\frac{r^2}{r_s^2} - e^2 \right)^{1/2} - 0.05 \right] + \frac{30000}{r^2} +$$

$$+ \frac{3.93 \times 4\pi \sqrt{1-e^2} G10^3}{e^2} \left[1 - \left(1 - \frac{e^2 r_s^2}{r^2} \right)^{1/2} \right] -$$

$$- \frac{0.02489 \times 8\pi \sqrt{1-e^2} G10^3 r^2}{3e^4} \left[1 - \left(1 + \frac{r_s^2 e^2}{2r^2} \right) \left(1 - \frac{r_s^2 e^2}{r^2} \right)^{1/2} \right] \text{km}^2 \text{sec}^{-2} \text{kpc}^{-1} \quad (4)$$

where $G = 4.3007 \times 10^{-6} (\text{km}^2 \text{sec}^{-2} \text{kpc} M_\odot^{-1})$.

The function $F(r)$ has a discontinuous second derivative at $r = r_s$.

b) M-model

This model is a generalization of «Toomre's (1963) model 1». In this model of the Galaxy, the gravitational potential $V(r, z)$ is

$$V(r, z) = G \sum_{i=1}^2 \frac{M_i}{[r^2 + [a_i + (z^2 + b_i^2)^{1/2}]^2]^{1/2}}, \quad (5)$$

where: $a_1 = 0$, $b_1 = 0.495$, $a_2 = 7.258$, $b_2 = 0.52$ (in kpc)

and: $M_1 = 0.205 \times 10^{11}$, $M_2 = 2.547 \times 10^{11}$.

The advantages of this model are: (a) It has no singularities, (b) it involves functions quite explicit and elementary, and (c) the corresponding density law represents very well the distribution of mass in real flat galactic systems (edge on galaxies). By using models of the form (5) we can avoid the singularities imposed by the superposition of spheroids in the central parts of Toome's flat models, as it was done by Shu et al. (1971 III), and by W. Roberts, M. Roberts and F. Shu (1975).

In the following we use several variants of the models S and M. Specifically, we do not necessarily take the parameters used by Schmidt

or Miyamoto-Nagai. In the figures we mark only those parameters which are different from those adopted by the above authors.

c) Spherical Halos

On the above models we superimpose spherical halos so that in a sphere of radius 20 kpc there exists a given amount of mass ($2 \times 10^{11} \odot$, $10^{11} \odot$, $0.7 \times 10^{11} \odot$, etc.) following three different density laws:

i) $\rho(r) = \text{constant}$

ii) $\rho(r) \sim r^{-1}$

iii) $\rho(r) \sim r^{-2}$

The curves of figures 1-10, refer to some of the most representative models, using different masses for the axisymmetric component and the halo and different density laws in the halo.

2. CLASSIFICATION OF THE ROTATION CURVES IN GALAXIES

The basic observational datum in the study of a galaxy is its rotation curve. Thus, it is worthwhile to examine the contribution in the rotation curve of each constituent of the galaxy (e.g. disk, halo, etc.), especially in the models M. In this way we can classify the galactic rotation curves according to the basic parameters of the distribution of mass in galaxies.

In the figures 1-4 we have considered the rotation curves based on several mass distribution drawn in all cases together with the rotation curve of the M-model (heavy line) which represents the rotation curve of our Galaxy. AM1 and AM2 are the «central» and «disk» masses, correspondingly, namely the masses which determine the form of the velocity curve in the central regions and in the intermediate distances.

The rotation curves in figure 1 have the same «disk» mass, while the «central» mass is varying.

If the central mass is small (e.g. $AM1 = 10^9 \odot$) the first peak in the rotation curve practically disappears while with $AM1 = 0.105 \times 10^{11} \odot$ it occurs lower than that in the M-model (heavy line) and with $AM1 = 0.305 \times 10^{11} \odot$ it occurs higher. If $AM1 = 0.105 \times 10^{11} \odot$, but the constant B1 is equal to 0.2 kpc (instead of $B1 = 0.495$ kpc as in the M-model) the peak becomes more acute and occurs higher and to the left than in

the M-model. It is obvious that the «central mass affects considerably the central part of the rotation curve ($r \leq 4 \text{ kpc}$), while it has small influence on the «disk» part of it.

In figure 2 we have removed the «central» mass. There are two sets of curves. In the first set (solid lines) we keep A_2 constant ($A_2 = 7.258 \text{ kpc}$) and we change only the mass AM_2 , while in the second set we keep constant the mass AM_2 , ($AM_2 = 2.547 \times 10^{11} \text{ } \odot$) and consider three values of A_2 . We note that in the first set the maxima occur for about the same value of r ($r = 11 \text{ kpc}$), while in the second set the maxima move to the left as A_2 decreases. What becomes obvious is that the rotation curves become higher either increasing the mass and keeping the «dimensions» of the disk component constant, or keeping the mass constant and decreasing the dimensions of the disk distribution. It is also worth noting that in the second set the curves converge to each other for large r to a much larger degree than in the first set. We have also tried the S-model with only the spheroidal distribution and found the same characteristics of the «disk» part of the rotation curve: an abrupt increase to a maximum and after that a smoother decrease - so that this form of the rotation curve seems to be characteristic of disc mass distributions.

In figure 3 we mark with HM, the halo mass inside a sphere of radius 20 kpc, considering in this case a density law $\rho \sim r^{-2}$. With the exception of the top curve where $HM = 0.9 \times 10^{11} \text{ } \odot$ the other three curves have been drawn with $HM = 0.7 \times 10^{11} \text{ } \odot$, while different combinations of the masses AM_1 , AM_2 have been examined, as indicated in the figure.

We have considered in figure 3 also several combinations of disk and halo masses with density law of the halo mass, $\rho \sim r^{-1}$. What is remarkable here is the fact that with a density law $\rho \sim r^{-1}$ the rotation curves become appreciably flat for large r , while in the case of a density law $\rho \sim r^{-2}$ the slope of the curves (for the same r) remains more or less constant. This can be easily explained by the fact that in a pure halo with density law as $\rho \sim r^{-2}$ the rotation curve is a straight line parallel to the r -axis, while in the case of the law r^{-1} it increases like a parabola (concave towards the r -axis). Therefore, the contribution in the flattening of the outerparts of the resultant rotation curve is much stronger in the second case than in the first.

In accordance to the previous considerations one could classify

the rotation curves of galaxies in terms of the distribution of mass as follows:

- I. If there is a significant amount of mass in the central region of flat galaxies, then the rotation curve has a first acute peak for small galactocentric distances.
- II. If the central and the halo mass are negligible then the rotation curve is characterized by an increase to a maximum and after that a smoother decrease.
- III. If the density of the halo mass follows the law r^{-1} , then the «disk» part of the rotation curve becomes flat, after it has reached a maximum. If the density of the halo mass follows the law r^{-2} , then the rotation curve becomes higher than that of a pure disk mass, without significant change in its slope. Alternatively a flat rotation curve can be explained by a halo following the law r^{-2} if the contribution of the disk in the outer parts of the galaxy is insignificant. The flat part found in the rotation curve of M31, from optical observations by Rubin and Ford (1970) and verified from 21-cm studies (see Roberts and Rots, 1973 and their references), according to our previous classification could be explained assuming a «hollow» halo surrounding the galaxy in which the density follows the law r^{-2} .

3. THE INFLUENCE OF A HALO AND OF A CENTRAL MASS ON THE POSITIONS OF THE RESONANCES

The «relative frequency» ν , in the case of a two armed spiral galaxy, is defined by:

$$\nu = \frac{2(\Omega_s - \Omega)}{\kappa} \quad (6)$$

and gives the resonances in a galaxy. Here Ω_s is the angular velocity of the spiral pattern, Ω is the angular velocity of the stars and κ their epicyclic frequency.

Resonances occur when ν is a rational number, but the most important ones are when $\nu = -1$, $\nu = 0$, $\nu = +1$. In the first case we are referring to the inner Lindblad resonance, in the second to the particle resonance and in the third to the outer Lindblad resonance.

In figure 5 we have drawn the curves of ν versus r for several Ω_s , in the case of the pure S-model (continuous lines) and after introdu-

cing a halo (dashed lines). In all examined cases the halo curves are lower than those of the corresponding axisymmetric model. From these curves we derive the galactocentric distances of the various resonances.

In figure 6 we compare the curves giving the resonances of the S-model with those resulting from several halo masses. The curves of figure 6 marked with M1 are due to a halo mass $2 \times 10^{11} \odot$ and density law r^{-1} and the curves due to a halo mass $0.7 \times 10^{11} \odot$ and density law r^{-1} with M3. The resonances due to $2 \times 10^{11} \odot$ and $0.7 \times 10^{11} \odot$ homogeneous halo are marked with H1 and H7. The above halo masses are contained within a sphere of radius 20 kpc.

In figure 7 we have drawn the inner and the particle resonances for different values of the central mass, marked in the figure with CM. From the study of the curves of figure 6 it becomes obvious that the halo mass influences considerably the particle and even more the outer resonance, but it leaves the inner resonance practically unaffected. On the contrary (figure 7) the central mass influences much more the inner resonance.

In figure 8 we have drawn the inner and outer Lindblad resonances under several mass configurations as indicated in the figure, using the M-model. (We have drawn only the particle resonance of the original M-model in order to avoid confusion). The basic difference between the two models is that, in the case of the M-model, by removing the central mass, there is a specific Ω_s in each case, beyond which the inner resonance disappears. In the general case of two mass distributions of the M-model (without halo), there is again a limiting Ω_s , beyond which there is no inner Lindblad resonance, but the range of permissible Ω_s 's is much larger.

The behaviour of these curves can be explained as follows. The epicyclic frequency κ can be written in the form:

$$\kappa = \left(3 \frac{F}{r} + \frac{dF}{dr} \right)^{1/2} \text{ kmsec}^{-1} \text{ kpc}^{-1}. \quad (7)$$

So that:

$$\Omega - \frac{\kappa}{2} = \left(\frac{F}{r} \right)^{1/2} - \frac{1}{2} \left(3 \frac{F}{r} + \frac{dF}{dr} \right)^{1/2} \text{ kmsec}^{-1} \text{ kpc}^{-1} \quad (8)$$

where F is the force on the galactic plane

In the case of our two models we have:

a) S-model

In this model it is:

$$\lim_{r \rightarrow 0} \left(\Omega - \frac{\kappa}{2} \right) = \infty \quad (9)$$

The same result holds, if one takes into account the influence of a halo. Therefore, in the S-models the inner Lindblad resonance exists for all values of Ω_s . The result does not change, if the central mass has been removed (term $30000/r^2$ in the force).

b) M-Model

$$\Omega - \frac{\kappa}{2} = \left[\frac{GM_1}{(r^2 + c_1^2)^{3/2}} + \frac{GM_2}{(r^2 + c_2^2)^{3/2}} \right]^{1/2} - \frac{1}{2} \left[4 \left[\frac{GM_1}{(r^2 + c_1^2)^{2/3}} + \frac{GM_2}{(r^2 + c_2^2)^{2/3}} \right] - 3r^2 \left[\frac{GM_1}{(r^2 + c_1^2)^{5/2}} + \frac{GM_2}{(r^2 + c_2^2)^{5/2}} \right] \right]^{1/2} \quad (10)$$

where $c_1 = a_1 + b_1$, $c_2 = a_2 + b_2$.

If there is no central mass ($M_1=0$) the maximum $(\Omega - \frac{\kappa}{2})_{\max}$ occurs for somewhat large value of r (around $r=10$ kpc) and is of the order of $(\Omega - \frac{\kappa}{2})_{\max} = 8 \text{ kmsec}^{-1} \text{ kpc}^{-1}$. On the other hand if $M_1 = 0$ the maximum of $\Omega - \frac{\kappa}{2}$ occurs much closer to the origin and $(\Omega - \frac{\kappa}{2})_{\max}$ is much larger.

As an example in the case of the pure M-model it is $(\Omega - \frac{\kappa}{2})_{\max} = 110 \text{ kmsec}^{-1} \text{ kpc}^{-1}$ at $r=0.61$ kpc. It is obvious that if $\Omega_s > (\Omega - \frac{\kappa}{2})_{\max}$ the equation $\Omega - \frac{\kappa}{2} = \Omega_s$ has no solution, i.e. there is no inner Lindblad resonance. It can be verified that as $r \rightarrow 0$ the curve $\Omega - \frac{\kappa}{2}$ tends to zero.

Considering halos superimposed on the M-model in which the density follows the law $\rho \sim r^{-1}$ or $\rho \sim r^{-2}$ a term of the form $cr^{-1/2}$ or cr^{-1}

(where c is a constant), is added correspondingly to $\Omega - \frac{\kappa}{2}$. Therefore, there is always an inner Lindblad resonance, since in this case $\Omega - \frac{\kappa}{2}$ tends to infinity as r tends to zero.

4. HALOS AND PITCH ANGLES OF SPIRAL ARMS

The dispersion relationships given by the theories of Lin-Shu and Lynden Bell-Kalnajs in the case of a two armed spiral galaxy are the following:

1) LIN-SHU

$$(Q_a x)^{1/2} = 2e^{-x} \sum_{n=1}^{\infty} \frac{I_n(x)}{1 - \nu^2/n^2} \quad (11)$$

where
$$x = \frac{k^2 \langle \dot{r}^2 \rangle}{\kappa^2} \quad (12)$$

2) LYNDEN BELL-KALNAJS

$$(Q_a x + Q_a^2 D)^{1/2} = 2e^{-x} \sum_{n=1}^{\infty} \frac{I_n(x)}{1 - \nu^2/n^2} \quad (13)$$

where
$$x = \left[k^2 + \left(\frac{4\Omega}{\kappa r} \right)^2 \right] \frac{\langle \dot{r}^2 \rangle}{\kappa^2} \quad (14)$$

$$D = \frac{1}{k_T^2 r^2} \left[4 - \left(\frac{4\Omega}{\kappa} \right)^2 \right] \quad (15)$$

and
$$Q_a = 0.2857 Q^2 \quad (16)$$

$$Q = \frac{\langle \dot{r}^2 \rangle^{1/2}}{\langle \dot{r}^2 \rangle^{1/2}_{\text{crit}}} \quad (17)$$

$$\langle \dot{r}^2 \rangle_{\text{crit}} = 0.2857 \frac{\kappa^2}{k_T^2} \quad (18)$$

$$k_T = \frac{\kappa^2}{2\pi G \sigma_0} \quad (19)$$

Here k is the wave number, Ω the angular velocity of the stars, κ their epicyclic frequency, r the galactocentric distance, $\langle \dot{r}^2 \rangle^{1/2}$ is the dispersion of radial velocities, whereas ν is the relative frequency which defines the resonances in a spiral galaxy.

We have called the quantity Q given by equ. (17) stability parameter. This is the ratio between the real dispersion of radial velocities to the critical value given by equ. (18) (Toomre, 1964). If a Lin-Shu type wave reaches corotation it is necessarily marginally stable ($Q=1$) at corotation. Finally k_T is the basic wave number connected with the critical value of the dispersion of radial velocities in order to have a stable disk against axisymmetric collapse. The surface density connected with k_T is σ_0 .

At any point of a spiral arm, the pitch angle is the angle γ between the spiral arm and the circle going through this point and is given by:

$$\gamma(r) = \tan^{-1} \left(\frac{2}{rk} \right) \quad (20)$$

in the case of a two-armed spiral. This angle determines the type of a spiral galaxy in Hubble's (1926) classification. The pitch angle of the spiral arms depends on:

1. the angular velocity Ω_s of the spiral pattern
2. the stability parameter Q
3. the halo mass, and
4. the axisymmetric model.

We have solved equ. (11) for three values of Ω_s (11, 12.5 and 14 $\text{kmsec}^{-1} \text{ kpc}^{-1}$) and for two values of the halo mass ($0.7 \times 10^{11} \text{ } \odot$, $2 \times 10^{11} \text{ } \odot$) inside a sphere of 20 kpc radius with density law $\rho \sim r^{-1}$. Here Q has been taken equal to unity. The resultant spiral arms are presented in figure 9. In all cases examined the spiral arms have been drawn from a point a little outside the inner Lindblad resonance up to the

particle resonance (only one spiral is given in order to avoid confusion). The first row corresponds to the pure S-model. It is obvious that the pitch angle decreases for smaller Ω_s 's and for larger masses in the halo. Indeed for the pure S-model at $r=10$ kpc, the values of the pitch angles for $\Omega_s=11$, 12.5 and 14 $\text{kmsec}^{-1} \text{kpc}^{-1}$ are $5^{\circ}6$, $7^{\circ}2$ and $8^{\circ}6$ correspondingly. On the other hand for $\Omega_s=14$ $\text{kmsec}^{-1}\text{kpc}^{-1}$ at $r=10\text{kpc}$ for a halo mass $\text{HM}=0.10^{11}_{\odot}$ the pitch angle is $7^{\circ}04$ while for $\text{HM}=2 \times 10^{11}_{\odot}$ it is $5^{\circ}3$.

The effect of the central mass is shown in figure 10, where we have drawn the spirals that correspond to three different values of the central mass (indicated in the figure by CM), in the S-model with $\Omega_s=12.5$ $\text{kmsec}^{-1}\text{kpc}^{-1}$. It is obvious that by increasing the central mass the spirals become more tightly wound. Thus, either a halo or a central mass produces a decrease in the pitch angle of the spiral arms. A discrimination between the two can be made by looking at the positions of the resonances.

The solutions of the Lynden Bell-Kalnajs dispersion relation (which are similar with Lin's solutions as regards the slope) depend on the angular velocity of the spiral pattern, on the halo (or central) mass, on the stability parameter, and on the axisymmetric model used, while the Lin-Shu are independent of the axisymmetric model and demand that at corotation Q must be unity.

In the work of W. Roberts, M. Roberts and F. Shu (1975) the form of the spiral arms depends only on the angular velocity of the spiral pattern and the distribution of the mass in accordance to the observed rotation curves in galaxies. However, these authors used only models without halo and with the stability parameter equal to unity ($Q=1$). This last restriction was necessary for them because they have used the Lin-Shu dispersion relation.

On the contrary using the Lynden Bell-Kalnajs dispersion relation we have found that the same pitch angle can be derived by different combinations of the angular velocity of the spiral pattern, the halo mass and the stability parameter (Terzides 1977).

5. CONCLUSIONS AND DISCUSSION

The conclusions of this work can be summarized as follows:

1. If we have from observations the rotation curve of a galaxy, the distribution of mass in the central region of the galaxy can be e-

established from the «central» part of the rotation curve. Therefore the contribution of the central mass to the dynamical behaviour of the galaxy is known. On the contrary the «disk part» of the rotation curve may be uncertain, since the same «disk part» of a rotation curve can be due either to a pure disk mass distribution or to a combination of a disk and a halo. In other words the same rotation curve can be reproduced by models consisting (besides the central mass) of either a pure disk mass distribution or a combination of a disk and a halo. Therefore the force, the potential, the angular velocity and the epicyclic frequency are the same in both types of models. But in the models with halo the surface density of the disk is smaller than the corresponding surface density of the models consisting of a pure disk mass distribution.

2. The halo influences more the positions of the particle and outer Lindblad resonance, whereas the central mass influences more the position of inner Lindblad resonance.

3. The pitch angle of the spiral arms due either to the Lin-Shu or to the Lynden Bell-Kalnajs dispersion relations depends on the angular velocity Ω_s of the spiral pattern, the stability parameter Q , the halo mass and the axisymmetric model. The pitch angle increases for either larger values of the angular velocity of spiral pattern Ω_s or for larger values of the stability parameter Q . On the other hand for models giving the same rotation curve (one with halo and the other without halo) the pitch angle of the spiral arms in the models with halo is smaller than the pitch angle in the models without halo.

We discuss the above conclusions:

From equs. (18) and (19) we have immediately that the critical value of the dispersion of radial velocities $\langle \dot{r} \rangle_{\text{crit}}^{1/2}$ is proportional to the ratio $\frac{\sigma}{\kappa}$. Therefore, whereas for the same galactocentric distance in both types of models (one with halo and the other without halo) giving the same rotation curve the epicyclic frequency is the same, the surface density in the model with halo is smaller than the value of the surface density in the model without halo.

As a consequence $\langle \dot{r} \rangle_{\text{crit}}^{1/2}$ in the first case is smaller than in the second, which means that the model with halo is more stable than the model without halo. Thus the stability parameter Q (for a certain galactocentric distance) in a model with a halo, is larger than in a model without a halo.

In general Q can be considered as function of the galactocentric distance and of the age of the stars, since stars of different ages have different dispersion of radial velocities. However, up to now we have no detailed information about the dispersion of radial velocities in the disks of external galaxies and in our Galaxy except in the vicinity of the sun.

The necessary and sufficient condition in order that the solutions of Lin-Shu dispersion relation reach corotation is that at corotation Q must be unity. If $Q < 1$ the galaxy is unstable towards axisymmetric collapse, while if $Q > 1$ the wave does not reach corotation and the excitation mechanism due to Lin is not applicable. If Q varies with r , then it cannot take arbitrary values (Terzides, 1977).

The pitch angle of the spiral arms depends on the halo and the angular velocity of the spiral pattern.

Since the solutions $x = x(\nu)$ of the Lin-Shu dispersion relation are independent of the model, the solutions $x = x(r)$, for a specific value of the angular velocity of the spiral pattern are the same for models giving the same rotation curve. But as becomes clear from equs. (18), (19) and (12) the wave number is conversely proportional of the surface density. That means that for a certain value of r , in a model with halo the wave number is (absolutely) larger than in a model without halo. Therefore in the first case the wave number curve $k = k(r)$ is higher than in the second one. Consequently the pitch angle of the spiral arms in the model with halo is smaller than the pitch angle in the model without halo.

As regards the dependence of the pitch angle of the spiral arms on the angular velocity of the spiral pattern Ω_s , we notice first that the relative frequency ν increases with Ω_s (see figure 5). On the other hand the values of the upper branch solution $x = x(\nu)$ of the Lin-Shu dispersion relation between inner Lindblad resonance and corotation decrease with increasing ν . Therefore the values of the variable x (and of k) decrease with increasing Ω_s , for the same distance r . As a consequence the pitch angle of the spiral arms increases with angular velocity of the spiral pattern.

ACKNOWLEDGEMENTS

The author wishes to thank Prof. G. Contopoulos for many useful suggestions and discussions. He is also thankful to Prof. B. Barbani for his encouragement.

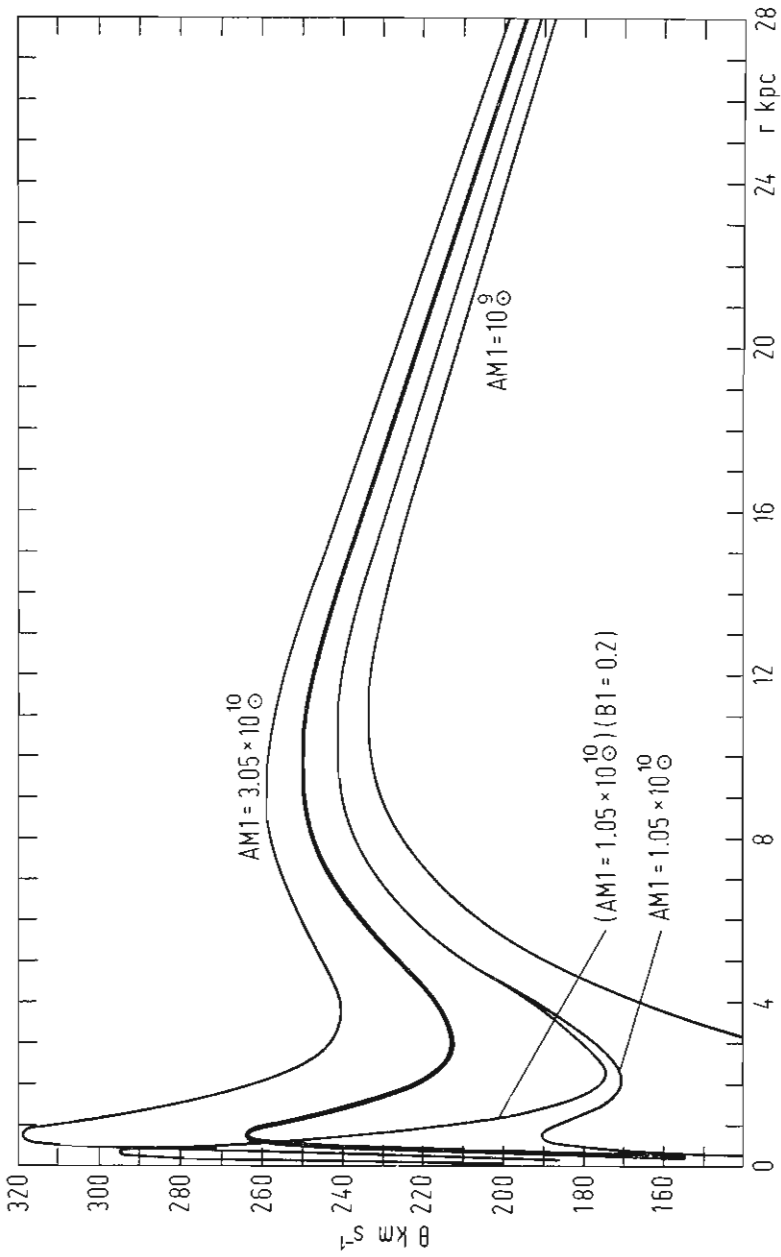


Fig. 1. Rotation curves due to models having the same «disk» mass, while the «central» mass is varying.

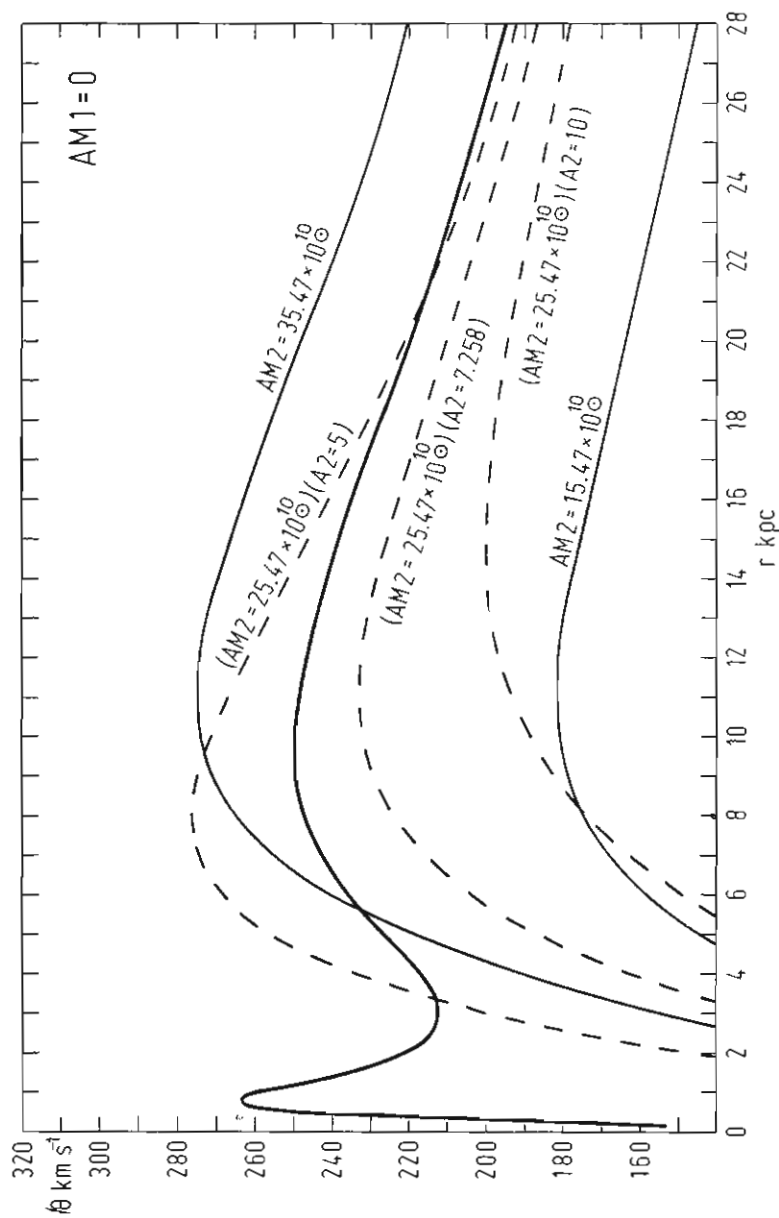


Fig. 2. The solid rotation curves are due to «disk» mass distributions of the same «dimensions» but the amount of mass is varying. The dashed rotation curves are due to models of the same «disk» mass distribution but of different «dimensions». In both cases the «central» mass is zero.

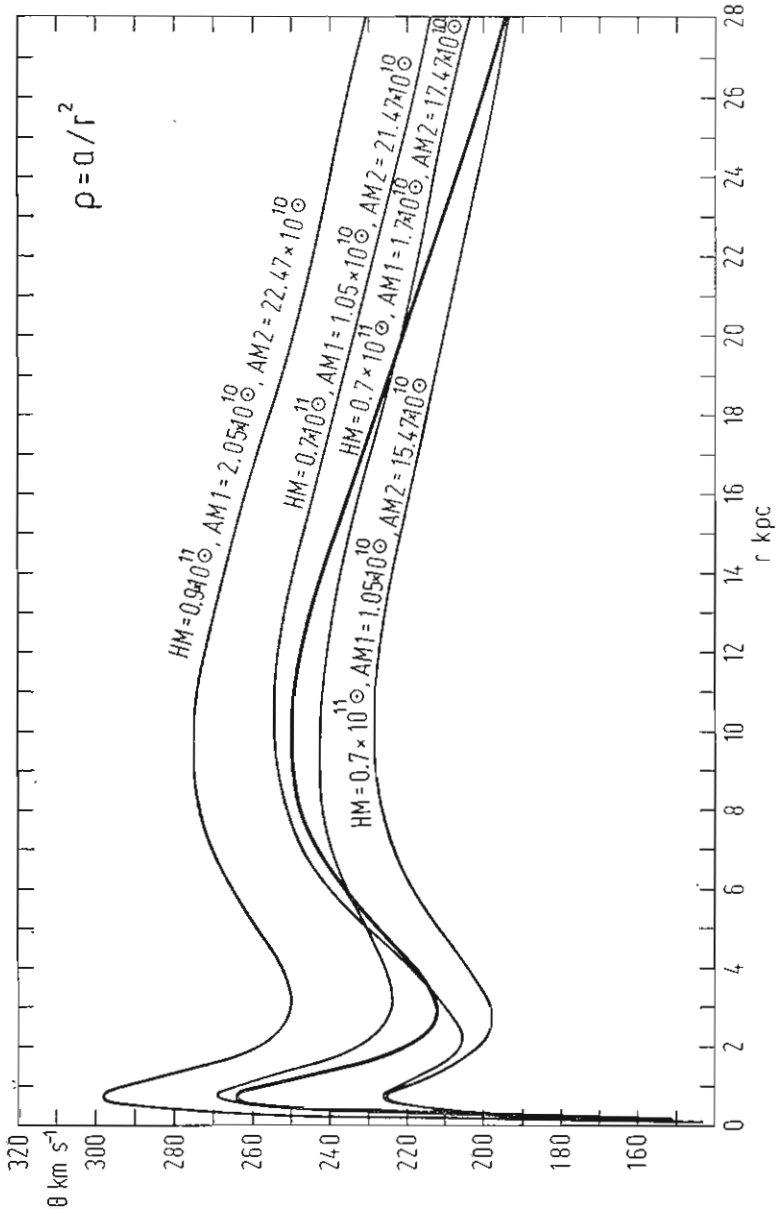


Fig. 3. Rotation curves due to M-models with density law $\rho = \frac{a}{r^2}$

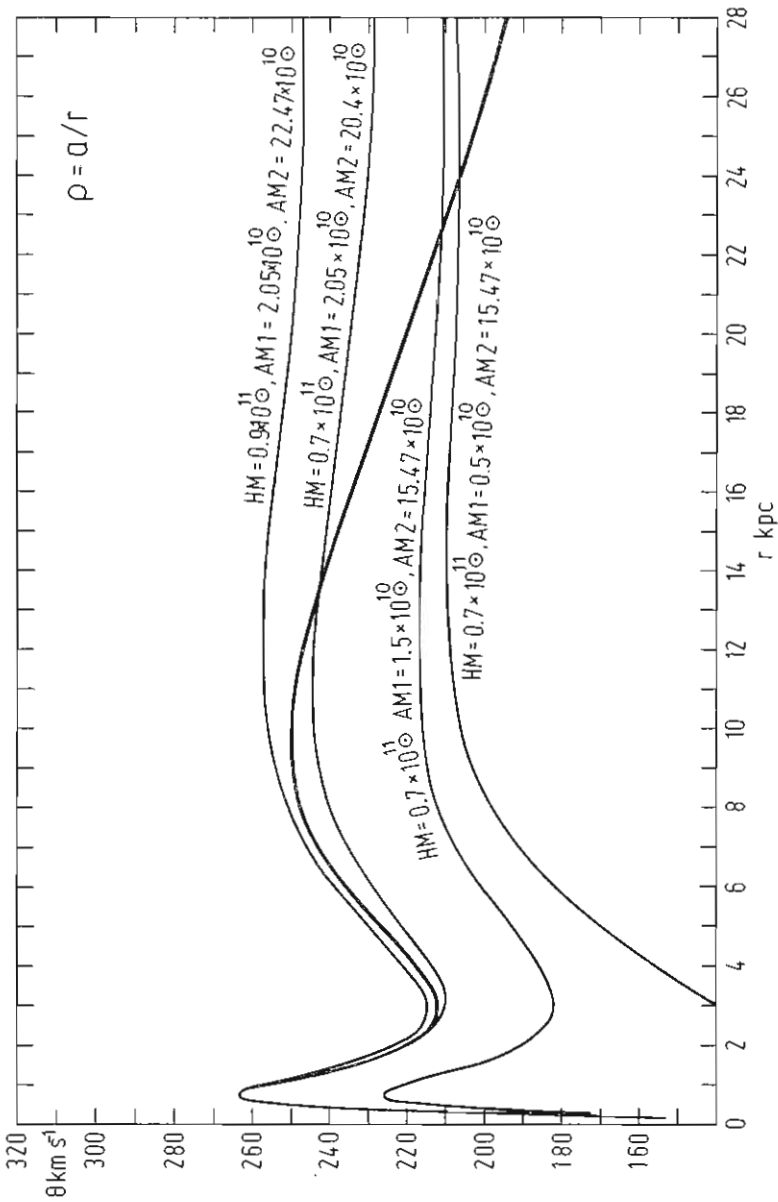


Fig. 4. Rotation curves due to M-models with halos with density law $\rho = \frac{a}{r}$

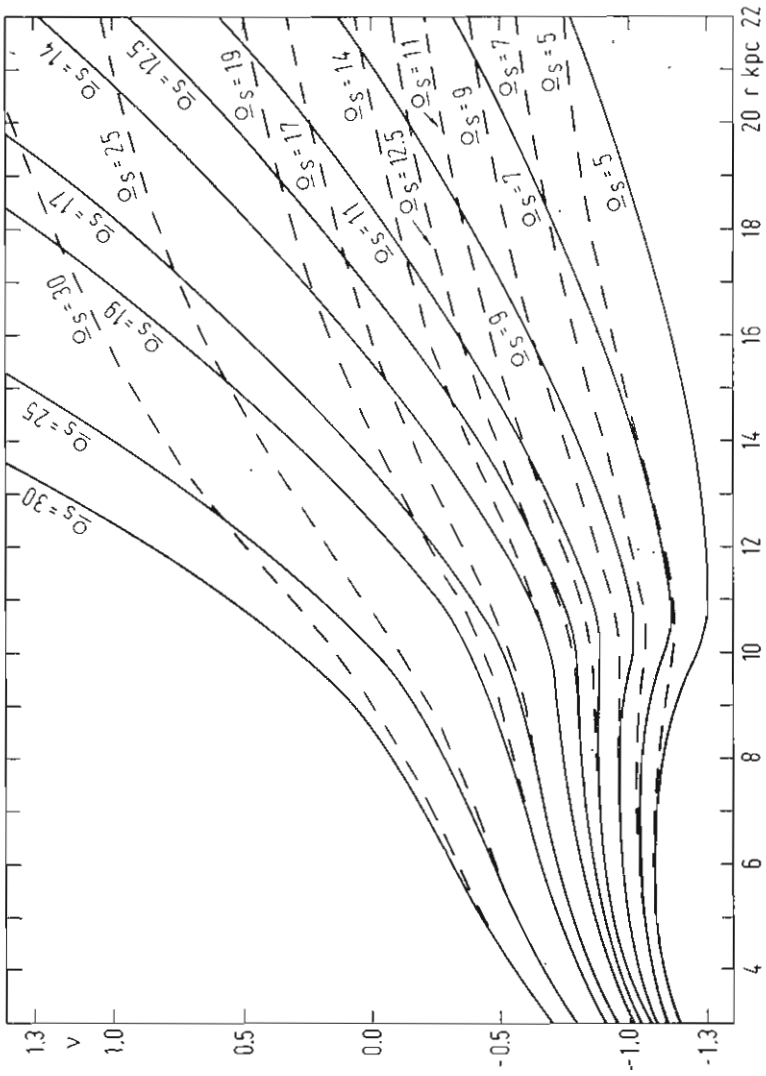


Fig. 5. The relative frequency ν given by eq. (6) versus r due to S-model (solid curves) and due to S-model + a homogeneous halo (dashed curves) for several values of the angular velocity of the spiral pattern Ω_s

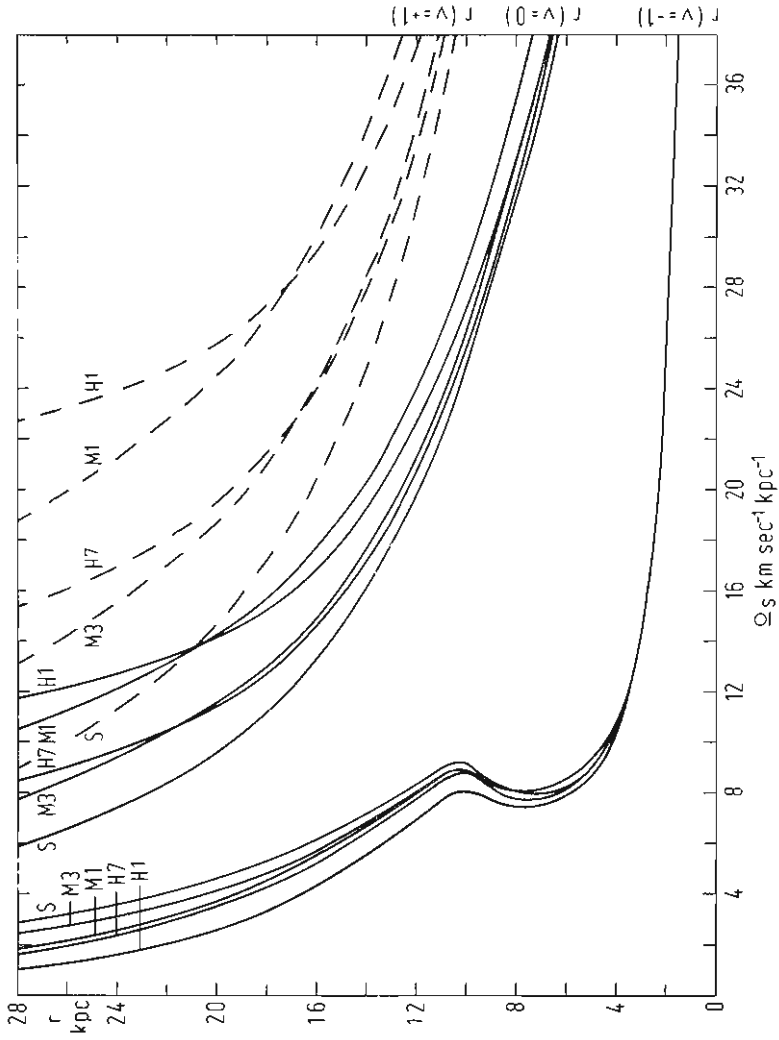


Fig. 6. The main resonances in the S-models for several halo masses.

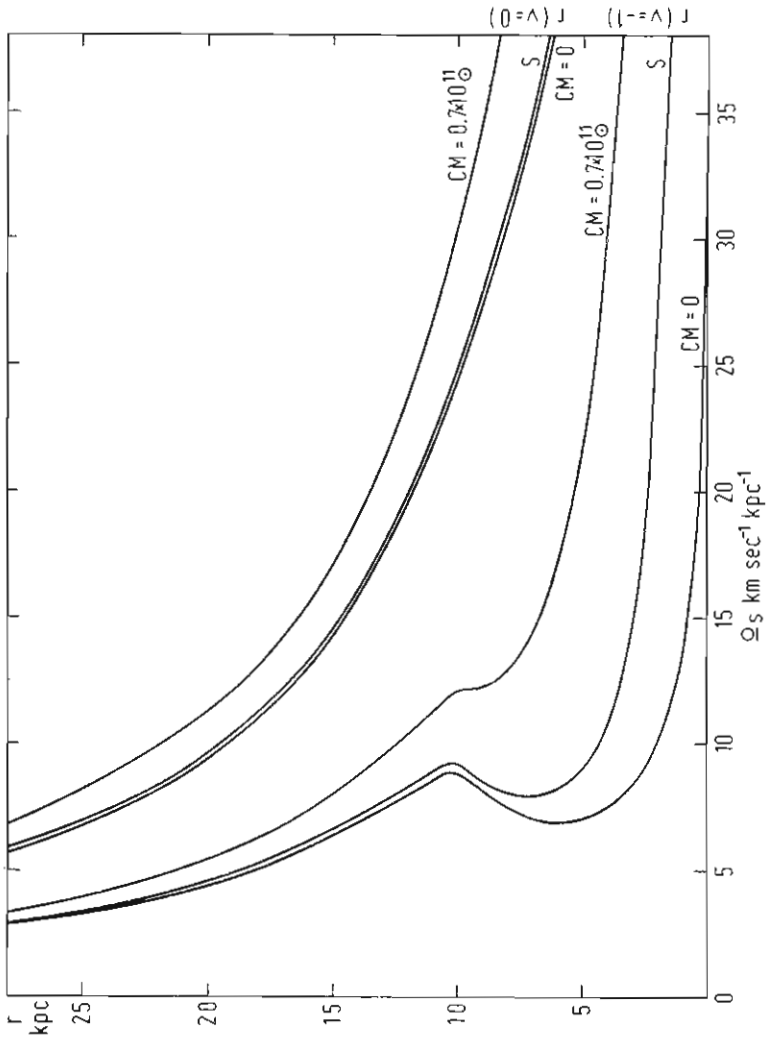


Fig. 7. The inner Lindblad resonance and particle resonance in the S-models for different central masses (marked with CM).

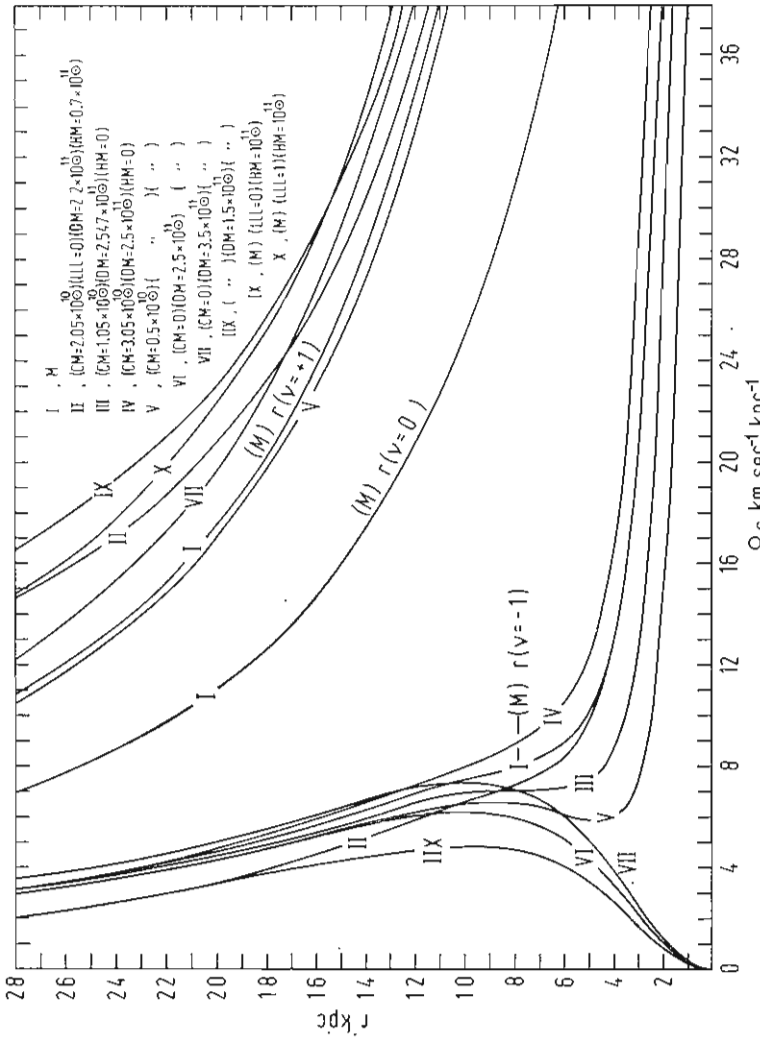


Fig. 8. The inner and outer Lindblad resonances in the M-models for several distributions of mass (only the particle resonance of the pure M-model is given); with CM is marked the central mass and with HM the halo mass. For LLL=0 the density law of the halo mass is $\rho = \frac{a}{r}$ while for LLL=1 it is $\rho = \frac{a}{r^2}$

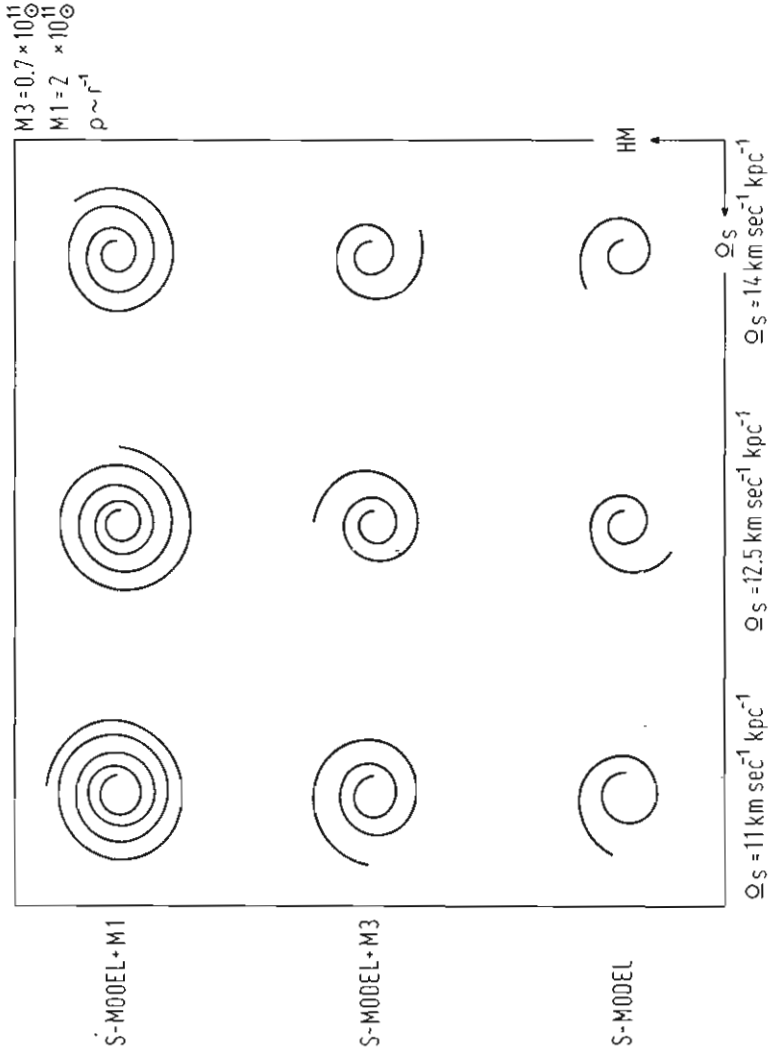


Fig. 9. The form of the spiral arms due to the Lin-Shu dispersion relation for various values of the angular velocity of the spiral pattern Ω_s and the halo mass.

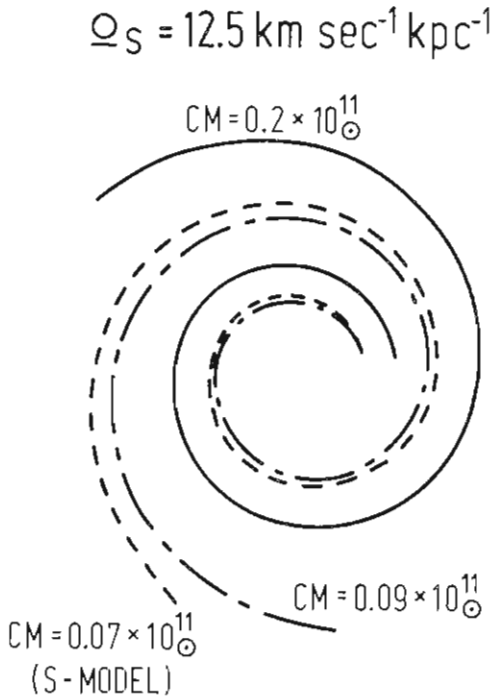


Fig. 10. The form of the spiral arms due to the Lin-Shu dispersion relation for various values of the central mass.

REFERENCES

1. CONTOPOULOS, G. 1972. «The Dynamics of Spiral Structure», Lecture Notes (College Park: University of Maryland, Astronomy Program).
2. CONTOPOULOS, G. 1973a, in Dynamical Structure and Evolution of Stellar Systems. Third Advanced course of the Swiss Soc. of Astr. and Astrophys., L. Martinet and M. Mayor, eds. (Geneva Observatory), p. 1.
3. — 1975, Private communication.
4. CHERNIN, A. D., J. EINASTO, E. SAAR, 1976, *Astroph. and Space Science* 39, 53.
5. EINASTO, J., A. KAASIK, E. SAAR, 1974, *Nature* 250, 309.
6. EINASTO, J., A. KAASIK, E. SAAR, 1974, *Nature* 252, 111.
7. HOCKNEY, R. W., D.R.K. BROWNRIGG, 1974, *M.N.R.A.S.* 167, 351.
8. HOHL, F. 1975, La dynamique des galaxies spirales, ed. L. Weliachew (Centre national de la recherche scientifique, Paris), p. 55.
9. HUBBLE, E. 1926, *Ap. J.* 64, 321.
10. LIN, C. C. and F. H. SHU, 1964, *Ap. J.* 140, 646.
11. LIN, C. C. and F. H. SHU, 1967, in *IAU Symposium No. 31*, p. 313.
12. LYNDEN BELL, D. 1970, in *IAU Symposium No. 38*, p. 331.
13. LYNDEN BELL, D. 1972, in «Galaxies and Relativistic Astrophysics», Vol. 3, B. Barbanis and J. D. Hadjidemeytriu (eds.), (Berlin-Heidelberg-New York), p. 114.
14. LYNDEN BELL D. and A. J. KALNAJS, 1972, *M.N.R.A.S.* 157, 1.
15. MILLER, R. H. 1974, *Ap. J.* 190, 539.
16. MIYAMOTO M. and R. NAGAI, 1975, *Publ. Astr. Soc. Japan* 27, 533.
17. OSTRIKER, J. P. and P.J.E., PEEBLES, 1973, *Ap. J.* 186, 467.
18. OSTRIKER, J. P., P.J.E. PEEBLES, and A. YAHIL, 1974, *ibid.* 193, L1-L4.
19. OSTRIKER, J. P. and T. X. THUAN, 1975, *ibid.* 202, 353.
20. ROBERTS, M. S. and A. H. ROTS, 1973, *Astr. and Ap.* 26, 483.
21. ROBERTS, W. W., M. S. ROBERTS, and F. H. SHU, 1975, *Ap. J.* 196, 381.
22. RUBIN, V. C. and W. K. FORD, 1970, *Ap. J.* 159, 379.
23. SCHMIDT, M. 1965, *Stars and Stellar Systems* 5, 513.
24. SCHMIDT M. 1965, *Ap. J.* 202, 22.
25. SHU, F. H. 1968, Ph. D. Thesis, Harvard University.
26. SHU, F. H. 1970b, *Ap. J.*, 160, 99.
27. SHU, F. H., R. V. STACNIC, and J. C. YOST, 1971 III, *Ap. J.* 166, 465.
28. TERZIDES, CH. K., Ph. D. THESIS, Bonn University.
29. TOOMRE, A. 1963, *Ap. J.* 138, 385.
30. TOOMRE, A. 1964, *ibid.* 139, 1217.
31. TOOMRE, A. 1969, *ibid.* 158, 899.

ΠΕΡΙΛΗΨΗ

ΕΠΙΔΡΑΣΗ ΤΗΣ ΜΑΖΑΣ ΤΗΣ ΑΛΩ ΣΤΗ ΔΥΝΑΜΙΚΗ ΤΗΣ ΣΠΕΙΡΟΕΙΔΟΥΣ ΔΟΜΗΣ

Υπό

X. Κ. ΤΡΕΖΙΔΗ

(Έργαστήριο Αστρονομίας Αριστοτελείου Παν/μίου Θεσ/νίκης)

Στή μελέτη αυτή εξετάζονται τὰ ἀποτελέσματα τὰ ὅποια προκύπτουν ἀπὸ τὴ δυναμικὴ ἐπίδραση τῆς μάζας τῆς ἄλω τῶν σπειροειδῶν γαλαξιδῶν.

Γίνεται ταξινόμηση τῶν καμπύλων περιστροφῆς (ποῦ ἀποτελοῦν τὸ βασικότερο στοιχεῖο ἀπὸ τὶς παρατηρήσεις) καὶ ἐρευνᾶται ἡ ἐξάρτηση τῶν θέσεων τῶν συντονισμῶν ἀπὸ τὴ μάζα τῆς ἄλω. Τέλος ἐξετάζεται ἡ δυναμικὴ ἐπίδραση τῆς μάζας αὐτῆς στὴ μορφή τῆς σπειροειδοῦς δομῆς τοῦ γαλαξία.

Τὰ βασικὰ συμπεράσματα ποῦ προκύπτουν ἀπὸ τὴ μελέτη αὐτὴ εἶναι τὰ ἑξῆς: 1) Ἐνῶ ἡ δυναμικὴ συνεισφορά τῆς μάζας τῶν κεντρικῶν περιοχῶν μπορεῖ νὰ ἐρμηνευτεῖ μονοσήμαντα ἀπὸ τὴ μορφή τῆς καμπύλης περιστροφῆς, τὰ «τμήματα τοῦ δίσκου» τῶν καμπύλων περιστροφῆς μπορεῖ νὰ ὀφείλονται σὲ διάφορους συνδιασμούς μαζῶν δίσκου καὶ ἄλω. 2) Ἡ ἄλω ἐπηρεάζει περισσότερο τὶς θέσεις τοῦ σωματιακοῦ συντονισμοῦ καὶ τοῦ ἐξωτερικοῦ συντονισμοῦ Lindblad ἐνῶ ἡ μάζα τῶν κεντρικῶν περιοχῶν ἐπηρεάζει βασικὰ τὴ θέση τοῦ ἐσωτερικοῦ συντονισμοῦ. 3) Ἡ μορφή τῶν σπειρῶν ἐξαρτᾶται ἀπὸ τὴ γωνιακὴ ταχύτητα περιστροφῆς Ω_s τοῦ σπειροειδοῦς πεδίου καὶ ἀπὸ τὸν δείκτη Q ὁ ὅποιος, χαρακτηρίζει τὴν ἀστάθεια τοῦ δίσκου τῶν σπειροειδῶν γαλαξιδῶν ἔτσι ὥστε σὲ μεγαλύτερες τιμὲς τῶν Ω_s καὶ Q νὰ ἀντιστοιχοῦν πλέον κλειστὲς σπεῖρες. Τέλος γιὰ μοντέλα τὰ ὅποια δίνουν τὴν ἴδια καμπύλη περιστροφῆς, οἱ σπεῖρες εἶναι πλέον κλειστὲς στὰ μοντέλα μὲ ἄλω ἀπὸ ὅτι εἶναι στὰ μοντέλα χωρὶς ἄλω.